

Shear and elongational flow behavior of acrylic thickener solutions. Part II: effect of gel content

Saeid Kheirandish · Ilshat Gubaydullin ·
Norbert Willenbacher

Received: 9 June 2008 / Accepted: 12 October 2008
© Springer-Verlag 2008

Abstract We have investigated the effect of crosslink density on shear and elongational flow properties of alkali-swelling acrylic thickener solutions using a mixing series of the two commercial thickeners Sterocoll FD and Sterocoll D as model system. Linear viscoelastic moduli show a smooth transition from weakly elastic to gel-like behavior. Steady shear data are very well described by a single mode Giesekus model at all mixing ratios. Extensional flow behavior has been characterized using the CaBER technique. Corresponding decay of filament diameter is also well fitted by the Giesekus model, except for the highest crosslink densities, when filament deformation is highly non-uniform, but the non-linearity parameter α , which is independent of the mixing ratio, is two orders of magnitude higher in shear compared to elongational flow. Shear relaxation times increase by orders of magnitude, but the characteristic elongational relaxation time decreases weakly, as gel content increases. Accordingly, variation of gel content is a valuable tool to adjust the low shear viscosity in a wide range while keeping extensional flow resistance essentially constant.

Keywords Steady shear · Oscillatory squeeze flow · Elongational flow · CaBER · Acrylate thickener · Crosslinking · Sol-gel transition

Introduction

A broad variety of technically or commercially relevant materials like coatings, adhesives, pharmaceuticals, or personal care products are formulated as complex, multiphase fluids. Besides the liquid continuous phase, these formulations include solid components like inorganic pigments and fillers or organic binder particles, droplets of immiscible fluids and active ingredients. But their flow behavior is often controlled by so-called rheology control agents or thickeners in order to provide the desired processing and application properties.

In many technical processes fluids are subject to complex flow fields including strong extensional components. Accordingly, not only shear but also extensional flow properties of the corresponding complex formulations have been investigated intensively with respect to processing or application properties, e.g. by Fernando et al. (2000), Stelter et al. (2002), Agarwal and Gupta (2002), James et al. (2003), or Tuladhar and Mackley (2008). Another area of research is the relationship between molecular properties especially of thickeners and their extensional flow properties. The dependence of extensional viscosity on polymer concentration, molecular weight, molecular stiffness, or solution elasticity has been studied for various synthetic and natural polymers, e.g. by Kennedy et al. (1995), Dexter (1996), Ng et al. (1996), Solomon and Muller (1996), Stelter et al. (2002), or Plog et al. (2005).

S. Kheirandish · N. Willenbacher (✉)
Institute of Mechanical Process Engineering and Mechanics,
University of Karlsruhe, 76128 Karlsruhe, Germany
e-mail: norbert.willenbacher@kit.edu

I. Gubaydullin
BASF SE, Polymer Research,
67076 Ludwigshafen, Germany

Present Address:
S. Kheirandish
Borealis Polyolefine GmbH, St.-Peters Str. 25,
4021 Linz, Austria

The determination of the elongational viscosity of low viscosity fluids (like coatings, inks, adhesives, or personal care products) with typical viscosity values in the range of 10–1,000 mPa s is still an experimental challenge. Various techniques like porous media flow, opposing jet rheometry, four-roll mills, entrance pressure loss measurements in capillary rheometry including converging channel flow or bubble-growth and bubble-collapse measurements have been employed so far (Macosko 1994). These different techniques cover different strain rate and viscosity ranges. But in general, the flow kinematics is not purely extensional. The flow can be temporally or spatially inhomogeneous, and only apparent extensional viscosities can be determined, comparison of data using different experimental techniques have to be compared cautiously (Ferguson et al. 1997). In filament stretching experiments (Sridhar and McKinley 2002) a constant strain rate is imposed on the fluid and the corresponding tensile stress is measured. Under certain constraints the fluid forms a slender cylindrical filament of uniform thickness, which is uniaxially stretched and the extensional viscosity can be determined as a function of strain rate and total strain. But this technique is typically used for fluids in the viscosity range well above 1 Pa s (Bhardwaj et al. 2007; Tripathi et al. 2006).

In this paper we use another filament thinning technique, namely capillary break-up extensional rheometry (CaBER) (Entov and Hinch 1997; Bazilevskii et al. 2001), in order to characterize the elongational flow properties of aqueous thickener solutions. In a CaBER experiment a fluid drop is exposed to an extensional step strain, thus forming a liquid filament. Subsequent necking of that liquid bridge is controlled by the balance of capillary and viscoelastic forces. Large extensional strains are attained as the filament necks down and finally breaks. The only measured quantity usually is the change in the midpoint diameter with time. The advantage of this method is its wide applicability to various kinds of fluids even with viscosities as low as 100 mPa s. However, neither strain rate nor stress can be controlled externally, but often very high total strains can be achieved. Various polymer solutions have been investigated using this technique all forming uniform cylindrical filaments, with homogeneous thinning and subsequent breakup (Stelter et al. 2000, 2002; Clasen et al. 2006; Bhardwaj et al. 2007). In these cases the tensile stress is directly related to the surface tension of the fluid, the strain rate is defined by the change in the filament diameter, and finally the extensional viscosity can be extracted as a function of total strain. However, the filament shape can

also be non-uniform for certain other fluids. Not only Newtonian fluids (McKinley and Tripathi 2000) but also many commercially relevant complex fluids like paper coating colors, adhesives or cosmetic emulsions exhibit non-uniform liquid bridges resulting in a filament shape with concave curvature. In these cases neither stress nor strain rate are temporarily or spatially constant. In general, the calculated viscosity data are transient and/or apparent values. But irrespective of these problems, the filament lifetime or the minimum filament diameter a fluid can support may be used as a quick laboratory test to be correlated to application or processing properties (Willenbacher 2004).

Polymers and polyelectrolytes are predominately used as thickeners for water-based formulations (Braun and Rosen 2000). This paper focuses on the class of acrylate ester copolymers synthesized in a classical emulsion polymerization process and accordingly provided as highly concentrated, aqueous dispersions (pH 2–3.5). Typically methacrylic acid, acrylic acid (AA), and ethylacrylate (EA) are the main monomers used in the commercial applications (Hager and Martin 1957; Miller 1960). These thickeners are widely used in all kinds of water-borne coating or adhesive formulations adjusted to pH values between 7 and 9. Upon neutralization, the weak acrylic or methacrylic acid groups dissociate which leads to polymer dissolution and development of thickening properties. Accordingly, these thickeners are often termed alkali swellable emulsion polymers (ASE). Their hydrophobically modified (HASE) counterparts belong to the so-called associative thickeners, since their rheological behavior is strongly controlled by the hydrophobic alkyl groups grafted onto the polymer backbone, which tend to form aggregates in aqueous solution.

The shear rheological properties of these HASE-type thickeners have been studied intensively (English et al. 1997; Abdala et al. 2004), mainly focusing on the effect of chain length and concentration of the hydrophobic side groups, but also on the backbone composition as well as overall concentration and molecular weight of the polymer. The association of side chains has been proven by fluorescence spectroscopy (Kumacheva et al. 1996). The strong shear-thinning behavior of HASE-type polymer solutions is attributed to the breakup of the side chain aggregates. In transient extensional flow experiments a pronounced maximum of the elongational viscosity as a function of strain rate is reported and the viscosity drop at high strain rates is again attributed to the breakup of associations among hydrophobic side chains (Kennedy et al. 1995; Tan et al. 2000).

Even in the absence of grafted hydrophobic side chains, aggregation of polymer chains is an issue for acrylic thickeners. These materials are assumed to be statistical copolymers of e.g. EA and AA monomers, and if the EA blocks are long enough they get “sticky” or “blocky” and can cause intra- as well intermolecular association. The existence of large supramolecular aggregates has been clearly evidenced by static as well as dynamic light-scattering experiments (Dai et al. 2000; Wang et al. 2005). In the first part of this paper (Kheirandish et al. 2008) we have shown that such aggregates dominate shear rheology of the solutions but hardly contribute to the elongational viscosity. In fact, these polymers stabilize filaments up to very high Hencky strains $\varepsilon \approx 7$ and exhibit severe strain hardening, but the ratio of longest elongational and shear relaxation times is $\lambda_E/\lambda_S < 0.1$ suggesting that the aggregates may not withstand strong elongational flows and do not contribute much to the elongational viscosity. Furthermore, this highlights, that a unified description of rheological phenomena in complex fluids based on continuum mechanical constitutive equations may be seriously aggravated by flow-induced structural changes.

Another important issue for the performance of ASE-type thickeners is crosslinking. The radical polymerization process not only leads to a broad molecular weight distribution, but also includes statistical branching and crosslinking. Accordingly weakly crosslinked, highly swollen microgel particles exist in these thickener solutions and contribute to their rheology. This microgel fraction can be controlled by additional copolymerization of a small amount of appropriated crosslinkers. Rheological evidence for microgel particles in HASE-type (English et al. 1999) and HEUR-type thickeners (Mewis et al. 2001) has been reported. But so far, this phenomenon has not been investigated systematically and no data are available for ASE-polymers.

The scope of this paper is to compare shear and elongational flow properties of ASE-type thickeners. In part one of this paper we have focused on the impact of aggregation among “sticky” EA blocks on rheology (Kheirandish et al. 2008). This second part deals with the effect of crosslinking and microgel content on shear and extensional flow properties. A mixing series of the two commercial polymers Sterocoll FD and Sterocoll D (BASF Aktiengesellschaft) is used as a model system, which allows for a systematic variation of the average crosslink density, since these two polymers mainly differ in the content of a crosslinkable comonomer, which is only present in Sterocoll D.

Experimental

Materials

Sterocoll® FD and Sterocoll® D (BASF SE, Ludwigshafen, Germany) are commercial alkali swellable thickeners for paper coating. These thickeners are based on a copolymer of ethylacrylate and (meth)acrylic with molar ratio of acrylate to acids of about 1:1. They are made from emulsion polymerization and are supplied as milky, aqueous dispersion with a solids content of 25% and a pH of 2.2–2.6. The main difference between Sterocoll® FD and Sterocoll® D is in a content of diethylenically unsaturated monomer used. Gel fraction and average crosslinking density of Sterocoll® D are significantly higher than those of Sterocoll® FD.

We have prepared aqueous solutions of Sterocoll® FD and D with concentrations of 5 wt.%. These solutions were stirred at room temperature for 48 h and adjusted to pH 8 by slowly adding 1 N NaOH. Subsequently, samples were equilibrated for at least 24 h. Polymer concentration was determined thermogravimetrically after neutralization. These stock solutions have been used to prepare mixtures with different mixing ratios (Sterocoll® D fraction of total polymer content: $x = 0, 0.2, 0.3, 0.4, 0.5, 0.6, 0.7, 0.8, 0.9, 1$). Mixtures were again stirred for 48 h and the equilibrated for at least 24 h prior to testing.

Methods

Rotational rheometry

A rotational rheometer Haake RS100 (Thermo Electron) equipped with a cone-plate measuring cell (diameter $d = 40$ mm, cone angle $\alpha = 0.01$ rad) was used to perform steady shear as well as small amplitude oscillatory shear experiments. The latter covered the frequency range from 0.01 to 100 rad/s. Strain sweeps at $\omega = 3.14$ rad/s were performed prior to each frequency sweep in order to identify the linear viscoelastic response regime. Temperature was controlled at $T = 20 \pm 0.2$ °C using a fluid thermostat.

Oscillatory squeeze flow

Oscillatory squeeze flow experiments were performed using a piezo-driven axial vibrator (Crassous et al. 2005; Kirschenmann 2003) customized at the Institute for Dynamic Material Testing (Ulm, Germany). In these experiments the sample is placed into a gap between

two stainless steel plates. The lower one is supported by a thin-walled quadratic copper tube carrying the piezo-elements which exert the vibrational motion and pick-up the response signal. This lower part of the device is surrounded by a double-walled cylinder allowing for circulation of a thermostating fluid and the sample temperature is controlled with an accuracy of ± 0.1 °C. The upper boundary of the gap is a thick metal lid, which provides complete sealing of the fluid. The instrument operates at a constant force amplitude and from the ratio of the dynamic displacement of the lower plate (amplitude ~ 5 nm) with and without fluid the complex squeeze stiffness K^* of the fluid is obtained which is directly related to the complex shear modulus G^* assuming no-slip boundary conditions (Kirschenmann 2003):

$$K^* = \frac{3\pi R^4}{2d^3} G^* \left/ \left(1 + \frac{\rho\omega d^3 R^2}{10G^*} + \dots \right) \right. \quad (1)$$

where ρ is the fluid density, R (here 10 mm) is the radius and d is the height of the gap. The denominator in Eq. 1 is a series expansion taking into account the inertia of the fluid in the gap. The determination of G^* strongly depends on the exact knowledge of d , which is determined by calibration using Newtonian liquids with viscosities between 1 and 2,000 mPa s. Gap heights between 15 and 100 μm have been used here. Additional contributions of finite compressibility of the fluid can be safely neglected for the soft ($G^* < 1000$ Pa) polymer solutions investigated here, but samples have to be degassed carefully in order to avoid artificial compressibility from entrapped air. Moduli G' or G'' in the range from 0.1 Pa to 10 kPa are accessible with the set-up described here.

Capillary break-up extensional rheometry

In a CaBER experiment (Bazilevskii et al. 2001; Entov and Hinch 1997) a fluid drop is placed between two plates and subsequently exposed to an extensional step strain thus forming a liquid filament. A CaBER 1 (Thermo Electron) extensional rheometer was used here, equipped with plates of diameter $d_c = 6$ mm. Plate separation was changed from $L_{\text{ini}} = 6$ mm to $L_{\text{fin}} = 16$ mm within 40 ms. This choice of parameters ensured that the initial filament diameter at the beginning of the filament thinning process was always between 1 and 1.5 mm for the fluids investigated here and thus capillary forces dominate over gravitational forces and the subsequent necking of that liquid bridge is controlled by the balance of capillary and visco-elastic forces. The only measured quantity during filament necking is the change in the midpoint diameter $D(t)$ with time, which

is monitored using a laser micrometer. Deformation of a fluid element at the axial midplane of the bridge is purely uniaxial. Large extensional strains are attained as the filament necks down and finally breaks. The theory for the kinetics of capillary thinning of fluid filaments has been discussed thoroughly (Entov and Hinch 1997). Here we have calculated strain rate $\dot{\varepsilon}$, tensile stress τ_E and apparent extensional viscosity η_E according to following simplified equations (Yesilata et al. 2006):

$$\dot{\varepsilon} = -\frac{2}{D(t)} \frac{dD(t)}{dt} \quad (2)$$

$$\tau_E = \frac{2\sigma}{D(t)} \quad (3)$$

$$\eta_E = -\frac{\sigma}{\frac{dD(t)}{dt}} \quad (4)$$

The time directly after cessation of the motion of the plate is defined as $t = 0$ and the corresponding filament diameter D_0 is used to calculate the Hencky strain with time $\varepsilon(t)$:

$$\varepsilon(t) = 2 \ln \left(\frac{D_0}{D(t)} \right) \quad (5)$$

In addition to the determination of the midpoint diameter $D(t)$ the full filament shape during the thinning and necking process was monitored using a high-speed camera Fastcam 1024 PCI (Photron) equipped with a macro zoom objective (Eneo Verifokal B 45 Z03 MV-MP, focal length, 45–160 mm) allowing for 0.3-fold to onefold magnification. Illumination was done with a white LED from the back. All CaBER experiments were performed at ambient temperature.

Viscoelastic models

Linear viscoelasticity

The linear viscoelastic behavior of the mixed Sterocoll FD and D solutions can be modeled using a continuous relaxation spectrum $H(\lambda)$ of the following form suggested by Baumgärtel, Schausberger and Winter (BSW) (Baumgaertel et al. 1990),

$$H(\lambda) = n_e G_0 \left[\left(\frac{\lambda}{\lambda_c} \right)^{-n_g} + \left(\frac{\lambda}{\lambda_{\text{max}}} \right)^{n_e} \right] \quad (6)$$

which can be directly used to calculate the relaxation modulus $G(t)$:

$$G(t) = \int_0^{\lambda_{\text{max}}} \frac{H(\lambda)}{\lambda} e^{-\frac{t}{\lambda}} d\lambda \quad (7)$$

We use this empirical spectrum to predict the dynamic mechanical data since it uses only three parameters, a nominal maximum relaxation time λ_{\max} , crossover relaxation time λ_c and plateau modulus G_0 , in order to compare the viscoelastic behavior of different samples. The exponents n_g and n_e are assumed constants in the original BSW spectrum and represent the slopes of the relaxation spectra at low and high relaxation times, respectively. For mixtures with Sterocoll D contents between 0.4 and 0.7 a two-mode BSW-type relaxation spectrum of the form

$$G(t) = \phi_1 G_1(t; G_{0,1}, \lambda_{\max,1}, \lambda_{C,1}) + (1 - \phi_1) G_2(t; G_{0,2}, \lambda_{\max,2}, \lambda_{C,2}) \quad (8)$$

has to be used to describe the respective G' , G'' data in the whole frequency range.

Non-linear viscoelasticity

The Giesekus constitutive equation (Giesekus 1982) is used here to describe the non-linear response of the thickener solutions in shear and elongational flow experiments. This model has been chosen, since it has been successfully applied to describe the shear and elongational flow behavior of entangled solutions of wormlike micelles (Yesilata et al. 2006), which show similar behavior in shear and CaBER experiments as the thickener solutions investigated here. For a two-mode model, the stress tensor τ is given by:

$$\tau = \sum_{i=1}^2 \tau_i + \tau_S \quad (9a)$$

The polymer and the solvent contributions of the stress tensor, τ_i and τ_S are related to the deformation tensor D according to:

$$\tau_i + \lambda_i \overset{\nabla}{\tau}_i + \frac{\alpha}{g_i} \tau_i^2 = 2g_i \lambda_i D \quad (9b)$$

$$\tau_S = 2\eta_S D \quad (9c)$$

with the characteristic relaxation times λ_i , the relaxation strength g_i , the solvent viscosity η_S and the upper convected Maxwell derivative $\overset{\nabla}{\tau}$:

$$\overset{\nabla}{\tau} = \dot{\tau} - \nabla v^T \tau - \tau \nabla v \quad (9d)$$

The third term on the left hand side of Eq.9b represents the non-linear material behavior, which is characterized by the parameter α (for $\alpha = 0$ the upper-convected Maxwell model is retained).

It is important to note that solvent viscosity for such systems can only be treated as a parameter also including contributions of dissolved molecules to the viscosity of medium and resembles essentially the high shear viscosity of the solution (Yesilata et al. 2006).

The fluid mechanical analysis of filament thinning in the CaBER experiment is based on the simplified approach suggested by Entov and Hinch (1997). Ignoring axial curvature effects and assuming a homogeneous, uniaxial elongational deformation the single-mode Giesekus constitutive equation results in a set of ordinary differential equations for τ_{zz} , τ_{rr} , and $\dot{\epsilon}$, which can be solved using appropriate initial conditions as described in detail by Yesilata and coworkers (2006).

This gives the dependence of D on time, which is then used in the kinematic CaBER relations (2–5) to obtain apparent elongational viscosities and elongation rates.

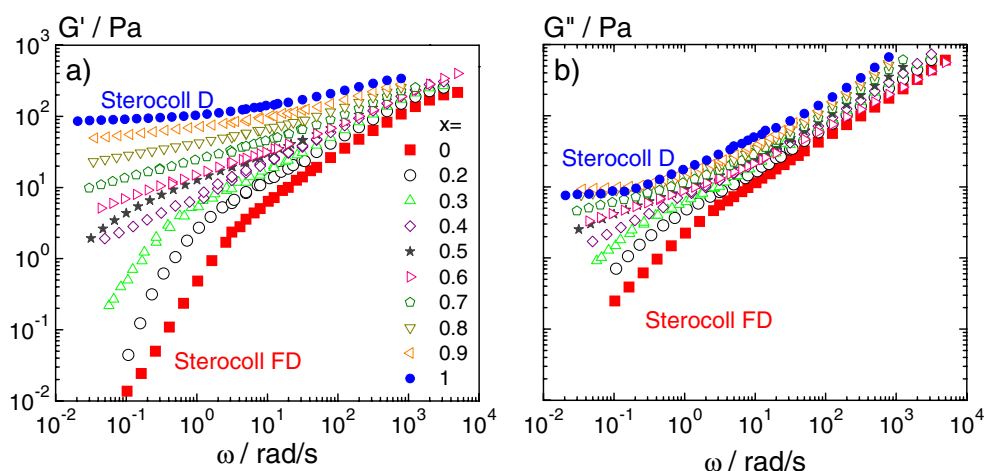
Results and discussion

Shear rheology

Figure 1a, b display the G' and G'' data obtained for all the solutions in the mixing series with constant total polymer concentration of 5% and various fractions of Sterocoll D ranging from 0 to 1. These data were obtained from small amplitude oscillatory shear and squeeze flow and cover the frequency range from 10^{-2} rad/s to 10^4 rad/s.

A gradual transition from predominantly viscous (pure Sterocoll FD) to highly elastic, gel-like behavior (Sterocoll D) is seen and the mixing series exhibits typical features of a sol-gel transition (Winter et al. 1988). The critical gel concentration is reached at a Sterocoll D content of 0.5 where G' equals G'' and both moduli follow a power-law $G' \sim G'' \sim \omega^\alpha$ with $\alpha = 0.4 \pm 0.05$ over an extended frequency range up to 10 rad/s. At higher frequencies local chain dynamics is prevailing and a characteristic Zimm-scaling ($\alpha = 0.588$) is observed irrespective of Sterocoll D content. In part one of this publication (Kheirandish et al. 2008) it has been demonstrated, that the relaxation of neutralized aqueous Sterocoll FD solutions with polymer concentrations between 0.5% and 5% follows the Zimm theory throughout the whole frequency range investigated. Obviously, the Zimm model fails when the crosslinked polymer Sterocoll D partly replaces Sterocoll FD. Instead, the whole set of data is very well described by the BSW-model as defined by Eqs. 6 and 7, at intermediate x -values a two-mode BSW-spectrum has to be used as given by Eq. 8. In contrast to the Zimm

Fig. 1 Storage modulus G' (a) and loss modulus G'' (b) at pH 8 for Sterocoll FD/Sterocoll D solutions with constant total polymer concentration of 5 wt.%, but different fractions of Sterocoll D as indicated in the graph



theory the BSW-model is purely phenomenological and does not include molecular parameters. Experimental data for $x = 0, 0.5,$ and 1 are compared to the fitted BSW-spectra in Fig. 2. All fit parameters are summarized in Table 1.

Results of steady shear experiments on the Sterocoll FD/Sterocoll D mixing series are shown in Fig. 3. As expected all the flow curves converge in the high shear regime, where the solution viscosity is determined by the stress relaxation of short chain segments and hence depends on polymer concentration but not on gel content and structure.

In contrast, stresses at low shear rates increase drastically with increasing gel fraction. This increase is particularly pronounced for $x > 0.5$. For $x > 0.7$ a

plateau in the $\tau - \dot{\gamma}$ curves develops corresponding to an apparent yield stress τ_y . Yield stress values vary from 1 Pa to 10 Pa as x increases from 0.7 to 1. The occurrence of an apparent yield stress is well-known for crosslinked acrylic thickeners and is attributed to a dense packing of the highly swollen gel particles (Braun and Rosen 2000). The parameters extracted from fitting the Giesekus model to the steady shear data according to Eqs. 9a–d are also summarized in Table 1. Although η_S is introduced as the solvent viscosity, the values from these fits are orders of magnitude higher than the true solvent viscosity here, and this quantity should be treated as a phenomenological parameter summarizing all Newtonian viscosity contributions. Essentially, η_S is the high shear limiting viscosity of the solutions also carrying contributions of solute molecules in the system. Similar observations have been reported by Yesilata et al. (2006). The characteristic longest relaxation times from steady and small amplitude oscillatory shear agree very well. Comparison with characteristic elongational relaxation times will be discussed below.

Extensional rheology

Figure 4 shows the results of the CaBER experiments performed on the solutions described above. The filament midpoint diameter is shown as a function of time. For the pure Sterocoll FD an almost ideal exponential decay is observed up to a very large deformation immediately before failure corresponding to a Hencky strain $\varepsilon \approx 7$. This has been discussed in more detail in the first part of this publication (Kheirandish et al. 2008). Similar behavior is found for all solutions of this mixing series up to $x = 0.5$ (data not shown), but the characteristic relaxation time decreases with increasing gel fraction and deviations from the Maxwell-type exponential

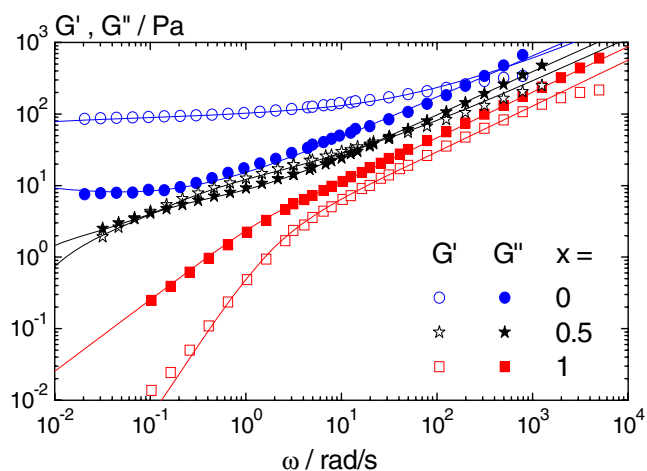


Fig. 2 Linear viscoelastic relaxation of polymer solutions with different Sterocoll D content x . Comparison of experimental G' (open symbols) and G'' (closed symbols) data to BSW spectra (lines)

Table 1 Parameters of the BSW and Giesekus models for aqueous solutions of Sterocoll FD and D with different fractions x of Sterocoll D (total polymer content 5 wt.%, pH 8)

| x | 0 | 0.2 | 0.3 | 0.4 | 0.5 | 0.6 | 0.7 | 0.8 | 0.9 | 1 |
|---|------|------|------|------|------|--------|------|-------|--------|---------|
| Small amplitude oscillatory shear—BSW model | | | | | | | | | | |
| $\lambda_{\max,1}/s$ | 0.96 | 1.69 | 30 | 80 | 150 | 300 | 800 | 1,200 | 10,000 | 100,000 |
| $\lambda_{C,1}/s$ | 0.66 | 0.65 | 0.75 | 0.4 | 0.43 | 0.43 | 0.43 | 0.21 | 0.13 | 0.08 |
| $G_{0,1}/Pa$ | 4.55 | 6.29 | 7 | 20 | 27 | 20.8 | 30 | 55 | 75 | 100 |
| $\lambda_{\max,2}/s$ | – | – | – | 15 | 8.7 | 3.5 | 3.5 | – | – | – |
| $\lambda_{C,2}/s$ | – | – | – | 3 | 0.24 | 0.0008 | 0.08 | – | – | – |
| $G_{0,2}/Pa$ | – | – | – | 4 | 13 | 100 | 100 | – | – | – |
| n_e | 0.22 | 0.22 | 0.22 | 0.27 | 0.28 | 0.15 | 0.15 | 0.15 | 0.15 | 0.2 |
| n_g | 0.65 | 0.65 | 0.65 | 0.58 | 0.61 | 0.59 | 0.59 | 0.59 | 0.59 | 0.58 |
| Steady shear—Giesekus model | | | | | | | | | | |
| α | 0.24 | 0.24 | 0.24 | 0.24 | 0.24 | 0.24 | 0.24 | 0.24 | 0.24 | 0.24 |
| $\eta_S/Pa \cdot s$ | 0.8 | 0.8 | 0.9 | 1 | 1.1 | 1.5 | 1.6 | 1.6 | 1.6 | 1.5 |
| λ_1/s | 0.65 | 1.15 | 25 | 80 | 120 | 300 | 700 | 850 | 1,000 | 2,500 |
| g_1/Pa | 4 | 4 | 0.45 | 0.5 | 0.7 | 0.75 | 1 | 2 | 3 | 5.4 |
| λ_2/s | – | – | 0.9 | 0.9 | 0.9 | 2 | 2 | 2 | 2 | 2 |
| g_2/Pa | – | – | 3 | 3 | 3.5 | 3 | 3 | 5 | 7 | 8 |
| Elongational deformation—Giesekus model | | | | | | | | | | |
| $\alpha/10^{-3}$ | 0.8 | 1 | 1.2 | 1.2 | 1.1 | 1.8 | 1.9 | 3.9 | 6.2 | – |
| $\eta_S/Pa \cdot s$ | 0.8 | 0.8 | 0.8 | 0.8 | 0.8 | 0.8 | 0.8 | 0.8 | 0.8 | – |
| λ_E/s | 0.27 | 0.27 | 0.26 | 0.25 | 0.24 | 0.22 | 0.2 | 0.16 | 0.12 | – |
| G_0/Pa | 4.5 | 2.3 | 2.2 | 2.1 | 1.8 | 1.6 | 1.6 | 1.55 | 1.2 | – |

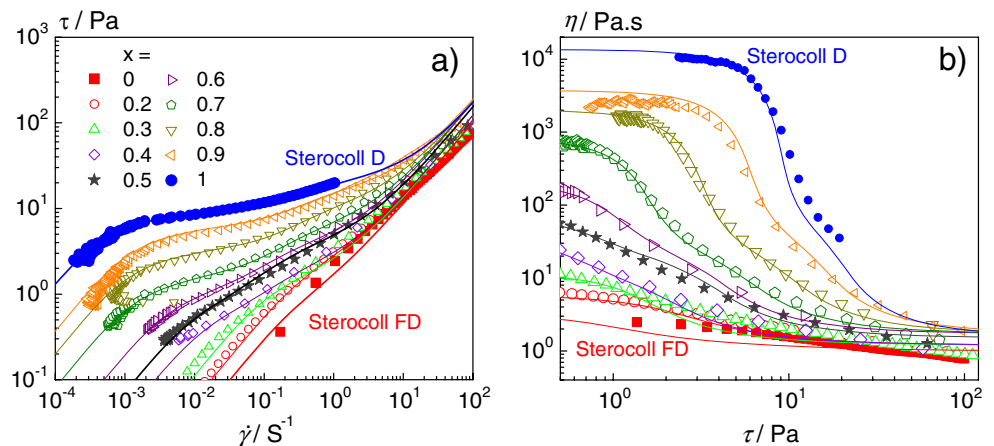
Giesekus model parameters for elongational deformation are according to Yesilata et al. (2006)

decay occur at slightly lower Hencky strains (for the solution with $x = 0.5$ e.g. at $\varepsilon \approx 6$). The time evolution of the filament diameter drastically changes for higher Sterocoll D fractions. The curves exhibit a pronounced downward bending and the convex curvature grows stronger with increasing x and accordingly the filament lifetime decreases by a factor of three going from $x=0$ to $x = 1$. Nevertheless, the diameter at failure is essentially the same for all solutions. This quantity is determined by the total polymer concentration as already pointed out in (Kheirandish et al. 2008) and does not depend on gel content. All data sets except that for the solution with $x = 1$, which shows a very sharp decay of

filament diameter, are well described by a single mode Giesekus model, the corresponding fit parameters are summarized in Table 1. This model includes a non-linearity parameter α , which increases almost by one order of magnitude when x increases from 0 to 0.9 in CaBER experiments, while constant value of $\alpha = 0.24$ has to be used in order to fit the steady shear data. On the other hand, the values for η_s determined from shear and elongational flow experiments are very similar.

We have calculated the transient strain rates $\dot{\varepsilon}$ and the apparent extensional viscosities η_E directly from the experimental diameter vs. time curves according to Eqs. 2–4 using numerical derivatives. The results are

Fig. 3 Steady shear results for aqueous Sterocoll FD/Sterocoll D solutions with different fractions x of Sterocoll D as indicated in the graph, **a** shear stress versus shear rate, **b** viscosity versus shear rate. The lines indicate fits of the two-mode Giesekus model to the corresponding experimental data. Total polymer concentration 5 wt.%, pH 8



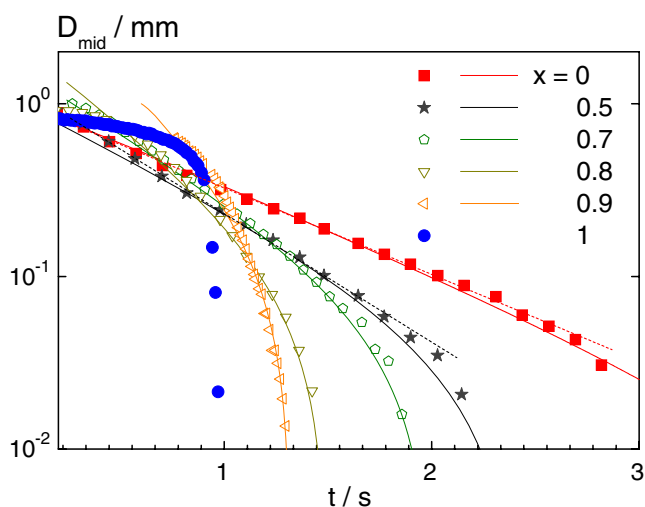


Fig. 4 CaBER experiments: filament midpoint diameter for solutions with content of Sterocoll D at a total polymer concentration 5% and pH 8. *Solid lines* correspond to a fit of the Giesekus model to the experimental data. *Dashed lines* indicate an exponential decay of filament diameter

shown in Fig. 5 together with the extensional viscosity data calculated from the Giesekus model using the parameters extracted from fitting the $D(t)$ curves. Up to a Sterocoll D content of $x = 0.5$ the mixed solutions exhibit severe strain hardening and an exponential increase in η_E at constant strain rates $\dot{\epsilon} \approx 3 - 4 \text{ s}^{-1}$. For the pure Sterocoll FD solution ($x = 0$) essentially no deviation from the ideal Maxwell behavior is observed until the filament breaks at $\epsilon = 7$. For the solution with $x = 0.5$ the strain rate $\dot{\epsilon}$ starts to increase monotonically for $\epsilon > 5.5$ and therefore, the corresponding leveling off in η_E cannot be interpreted in terms of an equilibrium limiting viscosity. The behavior of the solutions with $0 < x < 0.5$ (not shown here) is between that of the

solutions with $x = 0$ and $x = 0.5$. For the solutions with $x > 0.5$, $\dot{\epsilon}$ increases monotonically even at small deformations, and the transient elongational viscosity data are hard to compare with the results for the solutions with $x \leq 0.5$ or with results from other experimental techniques with different strain rate history. For the solution with $x = 0.9$, $\dot{\epsilon}$ increases by almost one order of magnitude until failure and the apparent extensional viscosity increases only weakly. For this solution we also observe a severe deviation in η_E calculated directly from the experimental $D(t)$ data and those calculated using the corresponding Giesekus model parameters, indicating that this model in the form we have used it here is not appropriate to describe the capillary thinning and break-up behavior of the solutions with high gel content.

The Giesekus constitutive equations as provided by Yesilata and coworkers (2006) are well suited to describe the CaBER experiments for Sterocoll solutions with $x \leq 0.8$ and have previously been applied successfully to characterize capillary thinning of entangled solutions of wormlike micelles (Yesilata et al. 2006), which show similar weakly bent $D(t)$ curves. One of the basic prerequisites for the derivation of these equations is the assumption of a homogeneously deformed cylindrical fluid filament. In order to check whether this assumption is fulfilled we have recorded the complete filament shape during the CaBER experiments using a high-speed camera. Images of filaments of solutions with $x \geq 0.5$ taken at similar midpoint diameter ($\approx 0.1 \text{ mm}$) are shown in Fig. 6. Obviously, the portion of the filaments, which is of uniform cylindrical shape, decreases strongly with increasing x . The filaments for the solutions with $x < 0.5$ (not shown here) exhibit the same almost ideal cylindrical shape as the $x = 0.5$ solution. Also the cylindrical portion of the filaments

Fig. 5 Apparent extensional viscosities η_E (a) and transient strain rates $\dot{\epsilon}$ (b) as calculated from the experimental $D(t)$ curves according to Eqs. 2–4 using numerical derivatives (symbols). η_E data as calculated from the Giesekus model using the parameters extracted from fitting the $D(t)$ curves (lines)

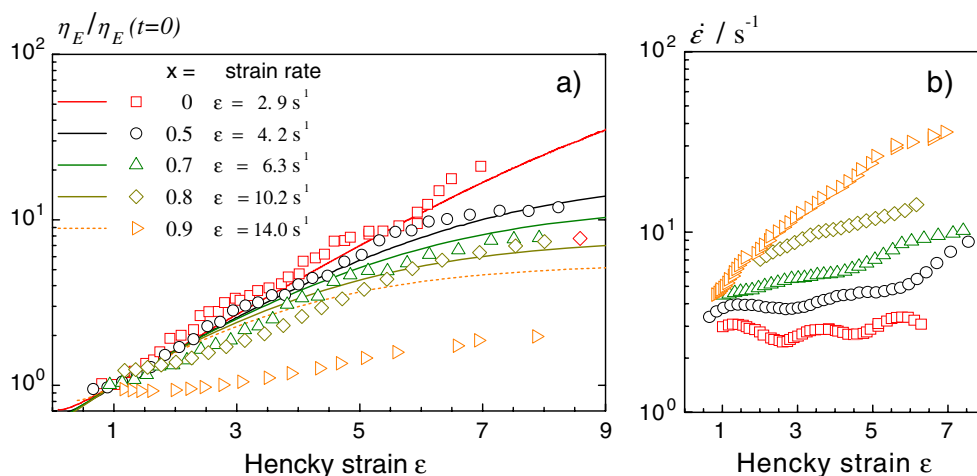
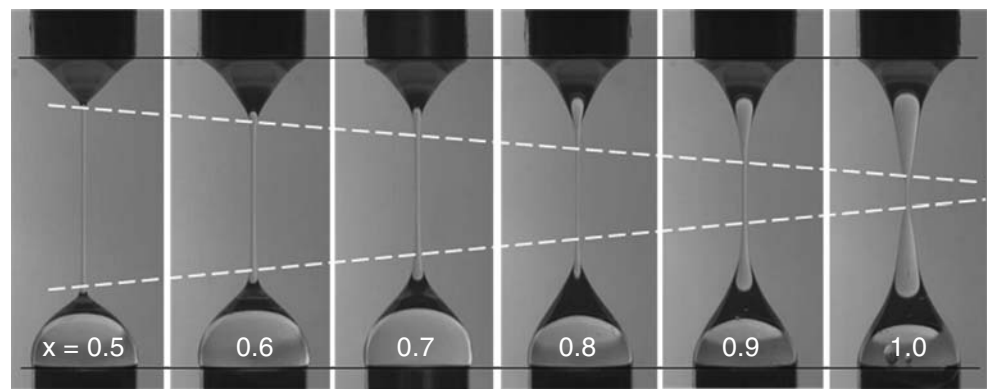


Fig. 6 Images of the complete filament shape in a CaBER experiment for Sterocoll FD/D solutions with $x \geq 0.5$ at similar midpoint diameter (≈ 0.1 mm). The dashed lines indicate the boundaries of the homogeneous cylindrical portions of the filaments



progressively decreases when x is increased from 0.5 to 0.8 the good fit of the Giesekus constitutive equations based on the cylindrical filament assumption suggests that these deviations are still not significant. For the pure Sterocoll D solution ($x = 1$) deformation takes place only in a narrow region of ± 1.3 mm around the point of minimum diameter. Moreover, filament failure seems to be induced by a necking process instead of a homogeneous filament thinning and the neck occurs not necessarily in the middle of the filament. Thus it is recommended to determine the filament diameter from image analysis of the filaments instead of using the laser micrometer, which is placed at a fixed position along the filament axis (usually in the centre of the filament) and averages the diameter over a width of 1 mm. On the other hand, non-uniform deformation and necking have also been observed in computational fluid dynamics simulations of the CaBER-type filament stretching process (Sujatha et al. 2008; Webster et al. 2008). These simulations reveal a pronounced necking at the filament midpoint for Giesekus fluids, which is not found if the experiment is simulated using linear Phan-Thien/Tanner or Oldroyd-B models. Moreover, the filament lifetime is shorter for Giesekus fluids and strain hardening is less pronounced compared to the other models if similar shear viscosity parameters are used. These qualitative similarities to our experimental results seem to suggest, that the Giesekus model is in fact appropriate constitutive equation to describe the flow behavior of the Sterocoll solutions investigated here. At this point it is important to note, that the non-linearity parameter α , which is essentially independent of the mixing ratio, is about two orders of magnitude lower in shear than in elongational flow. Therefore, these solutions cannot be termed “Giesekus fluids” since it is not clear which value for the parameter α would have to be used to describe their behavior in complex flow fields including variable contributions of shear and extension.

Moreover, it is not yet clear how far this continuum mechanical approach is valid at all, it might also be possible, that the final necking and filament break-up is controlled by the particulate nature of the weakly crosslinked gel fraction included in the solutions. An in-depth analysis of this break-up phenomenon would require additional experimental efforts and is beyond the scope of this paper.

Here we focus on the comparison of characteristic relaxation processes in shear and elongational flow. The corresponding longest relaxation times as obtained from steady and oscillatory shear as well as CaBER experiments are shown in Fig. 7. This comparison directly reveals, that the longest relaxations times obtained in the two different shear modes agree very well and increase by about four orders of magnitude upon increase of the gel content. In contrast, the characteristic elongational relaxation time decreases slightly (by less than a factor of 3) with increasing x . Even for the pure Sterocoll FD solution ($x = 0$) λ_E is significantly lower than $\lambda_{\max,s}$. This is attributed to the break-up of intermolecular aggregates, which are formed by attractive interactions among hydrophobic EA-sequences, in strong elongational flows and is discussed in detail in the first part of this paper (Kheirandish et al. 2008). The decrease in λ_E with increasing x is rationalized as follows: the gel particles, which more and more replace linear polymer chains or weakly bonded aggregates, can hardly deform and transmit tensile stresses and thus do not contribute much to the elongational flow resistance and stress relaxation. This is further supported by the very low value of the α parameters determined from the Giesekus analysis of the CaBER experiments. On the other hand, the deformation of gel particles and the sliding of the particles past each other dominates shear relaxation at small deformations and low shear rates. Accordingly, $\lambda_{\max,s}$ increases by orders of magnitude as x increases and the gel-particles are packed more densely.

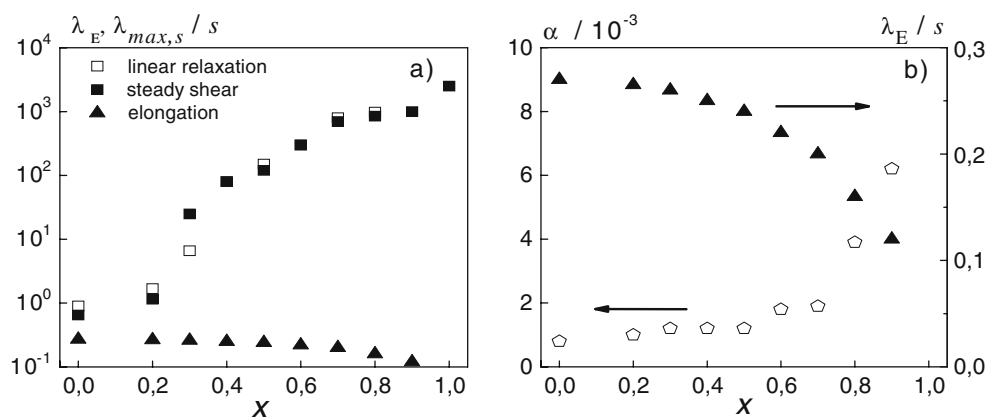


Fig. 7 **a** Characteristic relaxation times from shear (squares) and elongational rheometry (triangles). Open squares are the longest relaxation times obtained from small amplitude oscillatory shear ($\lambda_{max,1}$ in Table 1), filled squares are the longest relaxation times

obtained from a Giesekus analysis of steady shear data (λ_1 in Table 1). **b** elongational relaxation time λ_E (triangles) and Giesekus anisotropy parameter α (pentagons) from CaBER experiments, as a function of Sterocoll D content x

In conclusion, this demonstrates that the low shear viscosity of these acrylic thickeners can be varied in a wide range without affecting elongation flow resistance substantially just by variation of the gel content.

Conclusion

We have investigated the effect of crosslink density on shear and elongational flow properties of alkali-swelling acrylic thickener solutions using a mixing series of two commercial thickeners Sterocoll FD and Sterocoll D as a model system. Linear viscoelastic moduli show a smooth transition from weakly elastic to gel-like behavior. The data are well described by the phenomenological Baumgärtel–Schausberger–Winter model. A characteristic scaling behavior $G^* \sim \omega^\alpha$ with $\alpha = 0.4$ is observed at the so-called sol-gel transition, when a critical crosslink density is reached. The degree of shear-thinning in steady shear increases with increasing crosslink-density and an apparent yield stress is observed at the highest gel contents. These data are very well described by a single mode Giesekus model at all mixing ratios. Extensional flow behavior has been characterized using the CaBER technique. Solutions of the uncrosslinked Sterocoll FD form uniform cylindrical filaments, which thin homogeneously. With increasing crosslink density filament thinning is more and more restricted to the central part of the filament, but a uniformly thinning, cylindrical filament section is still maintained up to mixing ratios of 80% Sterocoll D. Moreover, the decay of the midpoint filament diameter is also well fitted by the Giesekus model. But for higher mixing ratios and especially for

pure Sterocoll D solutions, a sharp necking around the filament midpoint occurs and filament deformation is highly non-uniform. In these cases the simplified model (Yesilata et al. 2006) based on the assumption of a uniformly thinning, cylindrical filament fails. On the other hand, numerical simulations of the CaBER experiment using the Giesekus constitutive equation (Webster et al. 2008) reveal a strong necking around the filament midpoint, qualitatively similar to what is observed here. Nevertheless, it has to be pointed out, that the non-linearity parameter in shear is about two orders of magnitude larger than in elongational flow, and it is not clear how to apply the Giesekus model to describe the behavior of these thickener solutions in more complex flows with contributions of shear and extensional deformation. Finally, it is not yet clear, whether the continuum mechanical approach is still valid for these solutions, or whether the final necking and filament break-up process is controlled by the particulate nature of the weakly crosslinked gel fraction. Irrespective of these aspects of modeling the rheological behavior of the thickener solutions it can be stated, that the longest shear relaxation time increases by orders of magnitude as gel content increases, but the characteristic elongational relaxation time weakly decreases. In consequence, variation of gel content or crosslink density is a valuable tool to adjust the low shear viscosity in a wide range, while keeping the elongational flow resistance essentially constant.

Acknowledgements We thank Amit Kumar for his assistance in performing the CaBER experiments during his summer internship in Karlsruhe.

References

- Abdala AA, Wu W, Olsen KR, Jenkins RD, Tonelli AE, Khan SA (2004) Solution rheology of hydrophobically modified associative polymers: effects of backbone composition and hydrophobe concentration. *J Rheol* 48:979–994
- Agarwal S, Gupta RK (2002) An innovative extensional viscometer for low-viscosity and low-elasticity liquids. *Rheol Acta* 45:456–460
- Baumgaertel M, Schausberger A, Winter HH (1990) The relaxation of polymers with linear flexible chains of uniform length. *Rheol Acta* 29:400–408
- Bazilevskii AV, Entov VM, Rozhkov AN (2001) Breakup of an Oldroyd liquid bridge as a method for testing the rheological properties of polymer solutions. *Polym Sci Ser A* 43:716–726
- Bhardwaj A, Richter D, Chellamuthu M, Rothstein JP (2007) The effect of pre-shear on the extensional rheology of wormlike micelle solutions. *Rheol Acta* 46:861–875
- Braun DB, Rosen MR (2000) Rheology modifiers handbook, practical use & application. William Andrew, Norwich
- Clasen C, Plog JP, Kulicke WM, Owens M, Macosko C, Scriven LE, Verani M, McKinley GH (2006) How dilute are dilute solutions in extensional flows. *J Rheol* 50:849–881
- Crassous JJ, Régisser R, Ballauff M, Willenbacher N (2005) Characterization of the viscoelastic behavior of complex fluids using the piezoelectric axial vibrator. *J Rheol* 49:851–863
- Dai S, Tam KC, Jenkins RD (2000) Aggregation behavior of methacrylic acid/ethyl acrylate copolymer in dilute solutions. *Eur Polym J* 36:2671–2677
- Dexter RW (1996) Measurement of extensional viscosity of polymer solutions and its effects on atomization from a spray nozzle. *At Sprays* 6:167–191
- English RJ, Gulati HS, Jenkins RD, Khan SA (1997) Solution rheology of hydrophobically modified alkali soluble associative polymers. *J Rheol* 41:427–444
- English RJ, Raghavan SR, Jenkins RD, Khan SA (1999) Associative polymer bearing n-alkyl hydrophobes: rheological evidence for microgel-like behaviour. *J Rheol* 43:1175–1194
- Entov VM, Hinch EJ (1997) Effect of a spectrum of relaxation times on the capillary thinning of a filament of elastic liquid. *J Non-Newton Fluid Mech* 72:31–53
- Ferguson J, Hudson NE, Odriozola MA (1997) The interpretation of transient extensional viscosity data. *J Non-Newton Fluid Mech* 68:241–257
- Fernando RH, Xing LL, Glass JE (2000) Rheology parameters controlling spray atomization and roll misting behavior of waterborne coatings. *Prog Org Coat* 40:35–38
- Giesekus H (1982) A simple constitutive equation for polymer fluids based on the concept of deformation-dependent tensorial mobility. *J Non-Newton Fluid Mech* 11:69–109
- Hager O, Martin R (1957) Copolymer of acrylic acid ester, method of making, and use of said polymer to coat textile fabrics. US patent 3003987 and Martin and Hager (1957) Acrylic tetrapolymer and textiles coated with the same. US patent 3070561
- James DF, Yogachandran N, Roper JA III (2003) Fluid elasticity in extension, measured by a new technique, correlates with misting. 8th TAPPI Advanced coating fundamentals symposium, Chicago, pp 166–171
- Kennedy JC, Meadows J, Williams P (1995) Shear and extensional viscosity characteristics of a series of hydrophobically associating polyelectrolytes. *J Chem Soc Faraday Trans* 91:911–916
- Kheirandish S, Gubaydullin I, Wohlleben W, Willenbacher N (2008) Shear and elongational flow behavior of acrylic thickener solutions. Part I: Effect of intermolecular aggregation. *Rheol Acta*. doi:10.1007/s00397-008-0292-1
- Kirschenmann L (2003) PhD Thesis Institut für Dynamische Materialprüfung, Universität Ulm
- Kumacheva E, Rharbi Y, Winnik MA, Guo L, Tam KC, Jenkins RD (1996) Fluorescence studies of an alkaline swellable associative polymer in aqueous solution. *Langmuir* 12:182–186
- Macosko CW (1994) Rheology: principles, measurements and applications. Wiley-VCH
- McKinley GH, Tripathi A (2000) How to extract the Newtonian viscosity from capillary breakup measurements in a filament rheometer. *J Rheol* 44:653–670
- Mewis J, Kaffashi BG, Vermant J, Butera RJ (2001) Determining relaxation modes in flowing associative polymers using superposition flows. *Macromolecules* 34:1376–1383
- Miller (1960) Mineral coated paper products and methods of making them. US patent 3081198
- Ng SL, Mun RP, Boger DV, James DF (1996) Extensional viscosity measurements of dilute solutions of various polymers. *J Non-Newton Fluid Mech* 65:291–298
- Plog JP, Kulicke WM, Clasen C (2005) Influence of molar mass distribution on the elongational behavior of polymer solutions in capillary breakup. *Appl Rheol* 15:28–37
- Solomon MJ, Muller SJ (1996) The transient extensional behavior of polystyrene-based Boger fluids of varying solvent quality and molecular weight. *J Rheol* 40:837–856
- Sridhar T, McKinley GH (2002) Filament-stretching rheometry of complex fluids. *Annu Rev Fluid Mech* 34:375–415
- Stelzer M, Brenn G, Yarin AL, Singh RP, Durst F (2000) Validation and application of a novel elongational device for polymer solutions. *J Rheol* 44:595–616
- Stelzer M, Brenn G, Yarin AL, Singh RP, Durst F (2002) Investigation of the elongational behavior of polymer solutions by means of an elongational rheometer. *J Rheol* 46:507–527
- Sujatha KS, Matallah H, Banaai MJ, Webster MF (2008) Modeling step-strain filament-stretching (CaBER-type) using ALE techniques. *J Non-Newton Fluid Mech* 148:109–121
- Tan H, Tam KC, Tirtaamadja V, Jenkins RD, Bassett DR (2000) Extensional properties of model hydrophobically modified alkali-soluble associative (HASE) polymer solutions. *J Non-Newton Fluid Mech* 92:167–185
- Tripathi A, Tam KC, McKinley GH (2006) Rheology and dynamics of associative polymers in shear and extension: theory and experiments. *Macromolecules* 39:1981–1999
- Tuladhar TR, Mackley MR (2008) Filament stretching rheometry and break-up behaviour of low viscosity polymer solutions and inkjet fluids. *J Non-Newton Fluid Mech* 148:97–108
- Wang C, Tam KC, Tan CB (2005) Dissolution and swelling behaviors of random and cross-linked methacrylic acid-ethyl acrylate copolymers. *Langmuir* 21:4191–4199
- Webster MF, Matallah H, Sujatha KS, Banaai MJ (2008) Numerical modelling of step-strain for stretched filaments. *J Non-Newton Fluid Mech* 151:38–58
- Willenbacher N (2004) Elongational viscosity of aqueous thickener solutions from capillary break-up elongational rheometry (CaBER). *Proc XIVth Int Cong Rheol*, Seoul, S Korea
- Winter HH, Morganelli P, Chambon F (1988) Stoichiometry effects on rheology of model polyurethanes at the gel point. *Macromolecules* 21:532–535
- Yesilata B, Clasen C, McKinley GH (2006) Nonlinear shear and extensional flow dynamics of wormlike surfactant solutions. *J Non-Newton Fluid Mech* 133:73–90